

OPEN

MicroRNA Expression Signatures Associated With *BRAF*-Mutated Versus *KRAS*-Mutated Colorectal Cancers

Yong Won Choi, MD, Young Soo Song, MD, PhD, Hyunwoo Lee, MD, Kijong Yi, MD, Young-Bae Kim, MD, PhD, Kwang Wook Suh, MD, PhD, and Dakeun Lee, MD, PhD

Abstract: *BRAF* and *KRAS* genes are known to play a similar role in the activation of *RAS-RAF-MEK-ERK* signaling pathway in colorectal tumorigenesis. However, *BRAF*-mutated colorectal cancers (CRCs) have distinct clinicopathologic characteristics different from those of the *KRAS* mutated ones as in comparison the *BRAF*-mutated CRCs are associated with a much worse prognosis for the afflicted patients. This study aimed to determine the different miRNA expression signatures associated with *BRAF*-mutated CRCs in comparison to *KRAS*-mutated ones, and to identify the specific miRNAs possibly mediating the aggressive phenotype of the *BRAF*-mutated CRCs.

We screened 535 formalin-fixed paraffin-embedded CRC tissue samples for the *BRAF* V600E mutation, and selected 7 *BRAF*-mutated and 7 *KRAS*-mutated CRCs that were tumor size, stage, and microsatellite status-matched. Affymetrix GeneChip® miRNA 4.0 Array was used for detection of miRNA expression differences in the selected samples. We validated the array results by quantitative reverse transcription polymerase chain reaction (qRT-PCR) for selected miRNAs.

A total of 10 differentially expressed (DE) miRNAs associated with *BRAF*-mutated CRCs were obtained, including miR-31-5p, miR-877-5p, miR-362-5p, and miR-425-3p. miR-31-5p showed the highest fold change (8.3-fold) among all of the miRNAs analyzed. From the analyses of GO biological processes, the DE-miRNAs were functionally relevant to cellular proliferation such as positive regulation of gene expression ($P = 1.26 \times 10^{-10}$), transcription ($P = 9.70 \times 10^{-10}$), and RNA metabolic process ($P = 1.97 \times 10^{-9}$). Bioinformatics analysis showed that the DE-miRNAs were significantly enriched in cancer-associated pathways including neutrophin signaling ($P = 6.84 \times 10^{-5}$), pathways in cancer ($P = 0.0016$), Wnt signaling ($P = 0.0027$), and MAPK signaling pathway ($P = 0.0036$).

Our results suggest that the DE-miRNAs in *BRAF*-mutated CRCs in comparison to *KRAS*-mutated CRCs are implicated in the aggressive phenotype of the *BRAF*-mutated CRCs. Further experimental validation is required to confirm these results.

(*Medicine* 95(15):e3321)

Abbreviations: CRC = colorectal cancer, DE = differentially expressed, FDR = false discovery rate, FFPE = formalin-fixed paraffin-embedded, GO = gene ontology, KEGG = Kyoto Encyclopedia of Genes and Genomes, miRNA = microRNA, MSI = microsatellite instability, NCE = normal colon epithelium.

INTRODUCTION

Colorectal cancer (CRC) is the third most common cancer and the fourth for cancer-related deaths in the world population.¹ Despite recent multimodal treatments including radical resection with adjuvant chemoradiation therapy, the prognosis of the patients with metastatic disease has not improved greatly and the 5-year survival is less than 15%.² Recent targeted therapy, especially with antiepidermal growth factor receptor (anti-EGFR) antibodies may have significant therapeutic value, but only 10% to 20% of the patients with metastatic CRC benefit from such therapy.³ Currently, resistance to the EGFR-targeted monoclonal antibodies is largely ascribed to the *KRAS* mutations,⁴ and *BRAF* (V600E) mutation is also considered to be predictive of a negative response to EGFR inhibitors.^{5,6} As such, patients with CRCs harboring wild-type *KRAS* and *BRAF* are considered optimal candidates for EGFR therapies, and this categorization is thought to improve outcome and minimize unnecessary toxicity and cost for this subset of CRC patients.

KRAS mutations occur in about 35% to 45% of CRCs.^{7,8} The mutation of *BRAF*, kinase located downstream of *KRAS* in the EGFR signal transduction pathway, is found in about 10% to 15% of CRCs in the Western countries.^{9,10} The prevalence of *BRAF* mutation is much less in Asian countries, with only about 5% of the CRC cases.^{11,12} It is known that *KRAS* and *BRAF* gene mutations mostly occur in a mutually exclusive pattern, which has been interpreted as representing the functional redundancy of each mutation.¹³ Although both *KRAS* and *BRAF* genes are known to play a common role in the activation of *RAS-RAF-MEK-ERK* signaling pathway in colorectal tumorigenesis, unlike *KRAS*-mutated CRCs, *BRAF*-mutated ones have distinct clinicopathologic characteristics: they are tightly associated with the right-side colon, mucinous histology, CpG island methylator phenotype (CIMP), and/or microsatellite instability (MSI).^{9,10,14} More importantly, the *BRAF* mutation has been clearly associated with a poor prognosis.^{10,14} On the other hand, recent prospective trials demonstrated that *KRAS* mutation is not a prognostic marker for patients treated with adjuvant

Editor: Yong Liu.

Received: January 26, 2016; revised: March 10, 2016; accepted: March 14, 2016.

From the Department of Oncology and Haematology (YWC, HL), Department of Pathology (Y-BK, DL), Department of Surgery (KWS), Ajou University School of Medicine; Department of Pathology (YSS, KY), College of Medicine, and Department of Biomedical Informatics (YSS), Graduate School of Biomedical Science and Engineering, Hanyang University, Seoul, Republic of Korea.

Correspondence: Dakeun Lee, Department of Pathology, Ajou University School of Medicine, 164, Worldcup-ro, Yeongtong-gu, Suwon-si, Gyeonggi-do 443-380, Republic of Korea (e-mail: dakeun@gmail.com).

YWC and YSS contributed equally to this work.

This research was supported by Basic Science Research Program through the National Research Foundation of Korea (NRF) funded by the Ministry of Education (2014R1A1A1007905).

The authors have no conflicts of interest to disclose.

Supplemental Digital Content is available for this article.

Copyright © 2016 Wolters Kluwer Health, Inc. All rights reserved.

This is an open access article distributed under the Creative Commons Attribution-NonCommercial-NoDerivatives License 4.0, where it is permissible to download, share and reproduce the work in any medium, provided it is properly cited. The work cannot be changed in any way or used commercially.

ISSN: 0025-7974

DOI: 10.1097/MD.00000000000003321

5-FU-based chemotherapy.^{15,16} However, the reasons for these different clinicopathologic features of *KRAS*- and *BRAF*-mutated CRCs are largely unknown.

MicroRNAs (miRNAs), noncoding 18- to 25-nucleotide, are involved in various physiological processes through regulating the translation of genes.¹⁷ Altered miRNA expression levels and their significances in tumor initiation and progression have been reported in various human malignancies.^{18,19} Gene expression profiling studies have revealed that miRNA expression is an excellent biomarker associated with specific tumor subtypes and clinical outcomes.^{20,21} In CRCs, certain miRNAs such as miR-31 and miR-150 have been implicated in cancer development and progression.^{22–24} However, our understanding is limited on the different miRNA expression profiles of *BRAF*-mutated CRCs in comparison to *KRAS*-mutated CRCs. Previous studies investigated miRNA expression profiles only according to the *KRAS* or *BRAF* mutational status,^{25,26} and they did not consider other factors including rare cases of having both *KRAS* and *BRAF* mutations, histological subtypes, and MSI status of the tumors. Therefore, we aimed to determine the miRNA expression signatures associated with *BRAF*-mutated CRCs in comparison to *KRAS*-mutated ones, in order to identify specific miRNAs that may be indicative of the aggressive phenotype of *BRAF*-mutated CRCs.

MATERIALS AND METHODS

Patients and Tissue Samples

Five hundred eighty-three CRC patients who underwent curative surgery at Ajou University Hospital (Suwon, Republic of Korea) from October 2011 to April 2014 were initially considered for the study. After exclusion of 48 CRC patients with those having received neoadjuvant chemo- and/or radiotherapy ($n = 28$), having multiple occurrences ($n = 17$), and those with familial adenomatous polyposis ($n = 3$), a total of 535 CRC patients were enrolled for the further analysis. Corresponding formalin-fixed paraffin-embedded (FFPE) tissues for each patient was retrieved from the tumor registry. Clinicopathologic characteristics including age, gender, tumor size, tumor location, and TNM stage were obtained from electronic medical records. Tumor locations proximal to the splenic flexure were designated as “proximal,” and those located distal to the splenic flexure were labeled as “distal” for further analysis. Two gastrointestinal pathologists (YBK and DL) without background knowledge of the tissue samples performed microscopic characterization of the samples as tumor histology and differentiation. TNM stages were adjusted according to the AJCC 7th edition.²⁷ This study was carried out in accordance with the code of ethics of the World Medical Association (Declaration of Helsinki), and was approved by the Institutional Review Board (IRB) of Ajou University Hospital.

Genomic DNA Extraction

All the slides of the cases included in this study were reviewed, and the representative tumor blocks were selected for each case. Areas of the representative tumor were marked, and only the tumor tissue was gathered from 10- μ m thick sections of FFPE tissues by macrodissection. Genomic DNA was extracted from this tumor tissue using the ReliaPrep™ FFPE gDNA Miniprep system (Promega, Madison, WI). The concentration and purity of the extracted DNA were determined by a NanoDrop ND-1000 spectrophotometer (Thermo Fisher Scientific, Wilmington, DE). The extracted DNA was stored at -20°C until use.

Direct Sequencing for *BRAF* Mutation

The mutational analysis of *BRAF* exon 15 was performed by bidirectional sequencing of PCR fragments amplified from genomic DNA. PCR primers sequences and cycling conditions were as follows: exon 15 forward primer 5'-TGC TTGCTCTGATAGGAAAATG-3'; reverse primer 5'-TGATGG GACCCACTCCAT-3'; initial denaturation at 94°C for 15 minutes, followed by 40 cycles at 94°C for 30 seconds, 58°C for 30 seconds, and 72°C for 30 seconds and 1 cycle at 72°C for 5 minutes. After the amplified products were purified, direct DNA sequencing was performed using the Applied Biosystems 3500XL Genetic Analyzer with GeneMapper Software version 4.1 (Applied Biosystems, Life Technologies, Carlsbad, CA).

PNA Clamping Real-Time PCR for *KRAS* Mutation

The PNA Clamp *KRAS* Mutation Detection kit (PANA-GENE, Daejeon, Korea) was used to detect *KRAS* mutations in codon 12 and 13 by real-time PCR according to the manufacturer's instructions, as previously described.²⁸ Finally, ΔCt values were calculated as follows: $\Delta\text{Ct}1 = [\text{standard Ct}] - [\text{sample Ct}]$, and $\Delta\text{Ct}2 = [\text{sample Ct}] - [\text{non-PNA mix Ct}]$. A higher ΔCt value meant that the mutant was efficiently amplified. A cut-off value of 2.0 was used to determine the presence of mutant DNA.

Analysis for MSI

MSI analysis was performed with 5 microsatellite markers of the Bethesda consensus panel (D2S123, S17S250, D5S346, BAT25, and BAT26) as described previously.²⁹ From the National Cancer Institute recommendations, the tumors with instability at 2 or more microsatellite loci were defined as MSI-high (MSI-H), while the remaining cases were classified as microsatellite stable (MSS).

RNA Extraction and Quality Check

The miRNeasy FFPE Mini Kit (Qiagen, Valencia, CA) was used to extract total RNA, including miRNA, according to the manufacturer's instruction. The NanoDrop ND-1000 Spectrophotometer (Thermo Fisher Scientific) allowed quantification of RNA. For the quality control, RNA purity and integrity were evaluated by the OD 260/280 ratio, and analyzed by Agilent 2100 Bioanalyzer (Agilent Technologies, Palo Alto, CA).

Affymetrix miRNA Array Methods

The Affymetrix Genechip miRNA array processing was performed according to the manufacturer's protocol. RNA samples at 1 μg were labeled with the FlashTag Biotin RNA Labeling Kit (Genisphere, Hatfield, PA). The labeled RNA was quantified, fractionated, and hybridized to the miRNA microarray according to the standard procedures provided by the manufacturer. The labeled RNA was heated to 99°C for 5 minutes and then incubated at 45°C for 5 minutes. RNA-array hybridization was performed with agitation at 60 rotations per minute for 16 to 18 hours at 48°C on an Affymetrix 450 Fluidics Station (Affymetrix, Santa Clara, CA). The chips were washed and stained using a Genechip Fluidics Station 450 (Affymetrix). The chips were then scanned with an Affymetrix GeneChip Scanner 3000 (Affymetrix). Signal values were computed using the Affymetrix GeneChip Command Console software (Affymetrix).

Raw Data Preparation and Statistic Analysis

Raw data were extracted automatically in Affymetrix data extraction protocol using the software provided by Affymetrix GeneChip Command Console Software (AGCC) (Affymetrix). The CEL files import, miRNA level RMA + DABG-All analysis and result export using Affymetrix Expression Console Software. Array data were filtered by probes annotated species. The comparative analysis between test sample and control sample was carried out using fold-change and independent *T* test in which the null hypothesis was that no difference existed between the 2 groups. The miRNAs not detected in any samples were excluded from analysis. miRNAs not expressed completely in either group were also excluded. Significance of differential expression between two groups was estimated by *t* test for those miRNAs of at least a 1.5-fold reduced or increased mean expression between the 2 groups. All statistical tests of differentially expressed (DE) genes were conducted using the R statistical language v. 3.2.2. of the software.

Validation of Microarray Results by Quantitative Reverse Transcription Polymerase Chain Reaction (qRT-PCR)

Microarray expression results of the selected miRNAs including miR-31-5p, miR-362-5p, miR-425-3p, and miR-155-5p were verified by qRT-PCR. miR-155-5p was used as a negative control. Tissue RNA (1 µg) containing miRNA was polyadenylated with ATP by *E. coli* poly(A) polymerase (NEB) at 37°C for 30 minutes, before reverse transcription. Poly(A) tailed RNA (200 ng) was reverse transcribed to cDNA using PrimeScript Reverse transcriptase (Takara, Otsu, Japan) with oligo-dT adapter primer 5'-GCGAGCACAGAATTAATAC-GACTCACTATAGGTTTTTTTTTTT-3'. qRT-PCR was performed using RealHelix qPCR kit (Nanohelix) on CFX96 Touch Real time Detection System (Bio-Rad, Hercules, CA). The following primers were used in combination with the universal primer: U6, 5'-CTCGCTTCGGCAGCACA-3'; hsa-miR-31-5p, 5'-GCAGAGGCAAGATGCTG-3'; hsa-miR-362-5p, 5'-CGCA GAATCCTTGAACCT-3'; hsa-miR-425-3p, 5'-AGATCGG-GAATGTCGTGT-3'; hsa-miR-155-5p, 5'-TTAATGCTAATC GTGATAGGG-3'. Each sample was run in triplicates and the expression levels of miRNAs were normalized to an endogenous control RNU6B (U6). The relative expression levels of miRNAs were calculated by a comparative threshold cycle (Ct) method using the formula: $2^{-[\Delta Ct(\text{cancer}) - \Delta Ct(\text{normal colon})]}$.

Selection of High-Confidence miRNA Targets

To obtain high-confidence target genes of DE miRNAs, we combined target information from the most recent versions of four public databases (miRanda, TargetScan, miRDB, and TARBASE), applying cutoff of -0.1, -0.3, 60, and 0.8, respectively as suggested previously.³⁰⁻³² All the targets from TARBASE were considered high-confidence ones because they were experimentally validated. For the computationally predicted targets from the other 3 databases, only the targets predicted by at least 2 databases were considered to be high confidence ones.

Gene Ontology and KEGG Pathway Enrichment Analysis

To estimate the functions of DE miRNAs, we performed gene ontology (GO) and Kyoto Encyclopedia of Genes and Genomes (KEGG) pathway enrichment analysis using DAVID web application (<https://david.ncifcrf.gov>). High-confidence

targets were provided as an input to this tool. Internally, DAVID performs Fisher exact test to decide whether an input gene set is enriched for a specific gene set of GO terms or KEGG pathways compared to the background information. Only gene sets with $P < 0.05$ were considered significant when the false discovery rate (FDR) was less than 0.01 (for GO terms) or 0.2 (for KEGG pathway). Fold enrichment (FE) was used to estimate the enrichment degree of a given pathway, which is defined as follows:

$$FE = \frac{m/M}{n/N}$$

where *m* denotes the number of “hits” (mapped genes) in the pathway, *M* denotes the number of genes in the pathway, *n* denotes the number of “hits” in the background, and *N* denotes the number of total genes in the background. High score indicates more target genes in the corresponding pathway.

RESULTS

Selection of the Tumor Samples

Of the 535 patients initially enrolled in this study, we detected *BRAF*^{V600E} mutation in only 15 cases (2.8%). For strict comparative analysis matching histology and genetic alterations, the following *BRAF*-mutated cases were excluded from further analysis: 2 cases of mucinous adenocarcinomas with low tumor content, 2 early stage (T stage 1) small tumors arising from tubular adenoma, 3 cases with MSI-H, and 1 case with *KRAS* mutation. After exclusion of these 8 cases, the remaining 7 cases of *BRAF*-mutated CRCs were enrolled for the miRNA array analysis. For comparison, we selected another 7 tumors with MSS, T stage 2 and more, presence of *KRAS* mutation, and no *BRAF*^{V600E} mutation. The clinicopathologic characteristics of these 14 cases finally enrolled in this study are summarized in Table 1.

miRNA Expression Profiles of BRAF-Mutated CRCs in Comparison With KRAS-Mutated CRCs

The whole miRNA expression patterns in between *BRAF*-mutated and *KRAS*-mutated CRCs are shown in Figure 1. Comparative analysis of miRNA profiles between *BRAF*-mutated versus *KRAS*-mutated CRCs revealed a total of 31 DE-miRNAs. Unsupervised hierarchical clustering analysis demonstrated tumor clustering according to the *BRAF* mutational status (Figure 2). Among these miRNAs, only probesets corresponding to mature forms of miRNAs expressed in humans were selected for further analyses. Finally, we obtained a list of 10 miRNAs, which were significantly over- or underexpressed in *BRAF*-mutated cancers (Table 2). Among these, miR-31-5p, miR-877-5p, and miR-1237-5p were significantly up-regulated. On the other hand, let-7f-1-3p, miR-362-5p, miR-425-3p, miR-500a-5p, miR-532-5p, miR-660-5p, and miR-1825 were significantly downregulated in *BRAF*-mutated cancers. miR-532-5p had the highest fold change (-2.326-fold) among the down-regulated miRNAs, while miR-31-5p showed the highest fold change of 8.331 among all of these significantly altered miRNAs.

Validation of the miRNA Expression Profile by qRT-PCR

The differential expression detected by microarray analysis was evaluated by qRT-PCR for 3 selected miRNAs

TABLE 1. The Clinicopathologic Characteristics of 14 Patients With CRCs Either With *BRAF* or *KRAS* Mutation

| | <i>BRAF</i> -Mutated (n = 7) | <i>KRAS</i> -Mutated (n = 7) |
|---|------------------------------|------------------------------|
| Sex (male/female) | 3/4 | 4/3 |
| Age (mean, range), y | 67.6 (53–79) | 57.2 (43–82) |
| Tumor size (mean, range), cm | 5.3 (3.5–8) | 5.3 (3.5–8) |
| Tumor location (ascending/rectosigmoid) | 5/2 | 3/4 |
| Gross type (F/UF/UI) | 0/3/4 | 1/2/4 |
| Differentiation (MD/PD) | 3/4 | 6/1 |
| T stage (T2/T3/T4a)* | 0/4/3 | 1/6/0 |
| N stage (N0/N1a/N1b/N2a/N2b)* | 0/2/1/0/4 | 2/3/2/0/0 |
| Microsatellite instability (MSS/MSI-H) | 7/0 | 7/0 |

F = fungating, MSS = microsatellite stable, UF = ulcerofungating, UI = ulceroinfiltrative.

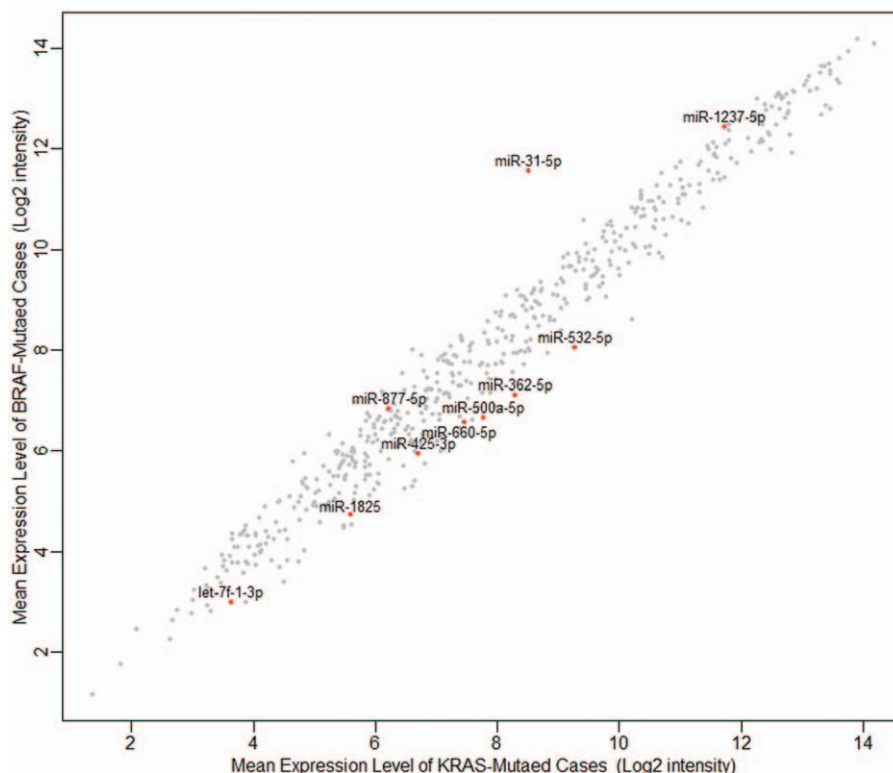
*T and N stages were defined according to the AJCC 7th ed.

(Figure 3). This experiment additionally included 14 cases of normal colon epithelium (NCE). In accordance with the array results, we observed significantly higher expression of miR-31-5p ($P = 0.008$) and significantly lower expression of miR-362-5p ($P < 0.001$) and miR-425-3p ($P = 0.001$) in *BRAF*-mutated CRCs in comparison to *KRAS*-mutated CRCs. We used miR-155-5p as a negative control since its expression level was similar in both groups by microarray, and we reached substantially the same results by qRT-PCR.

miRNA Targets and Relevant Biological Pathways

A total of 2408 target genes were predicted for the 10 miRNAs, and the network of miRNA-target genes was

constructed (Supplementary Figure 1, <http://links.lww.com/MD/A886>). When GO enrichment analysis were performed using DAVID, 41 GO terms were significantly enriched ($P < 0.05$), and 19 terms retained statistical significance by the Benjamini–Hochberg algorithm ($FDR < 0.01$). These 19 functional terms are summarized in Table 3. Our data revealed that functions relevant to cellular proliferation such as positive regulation of gene expression ($FDR = 5.00 \times 10^{-7}$), transcription ($FDR = 5.34 \times 10^{-7}$), and RNA metabolic process ($FDR = 1.31 \times 10^{-6}$) were distinctively associated. Further analyses of predicted target mRNAs of the DE-miRNAs revealed that 6 biologic pathways were significantly enriched ($FDR < 0.2$) in *BRAF*-mutated cancers in comparison to *KRAS*-

**FIGURE 1.** Scatter plot for the microRNA expression between *BRAF*-mutated and *KRAS*-mutated colorectal cancers.

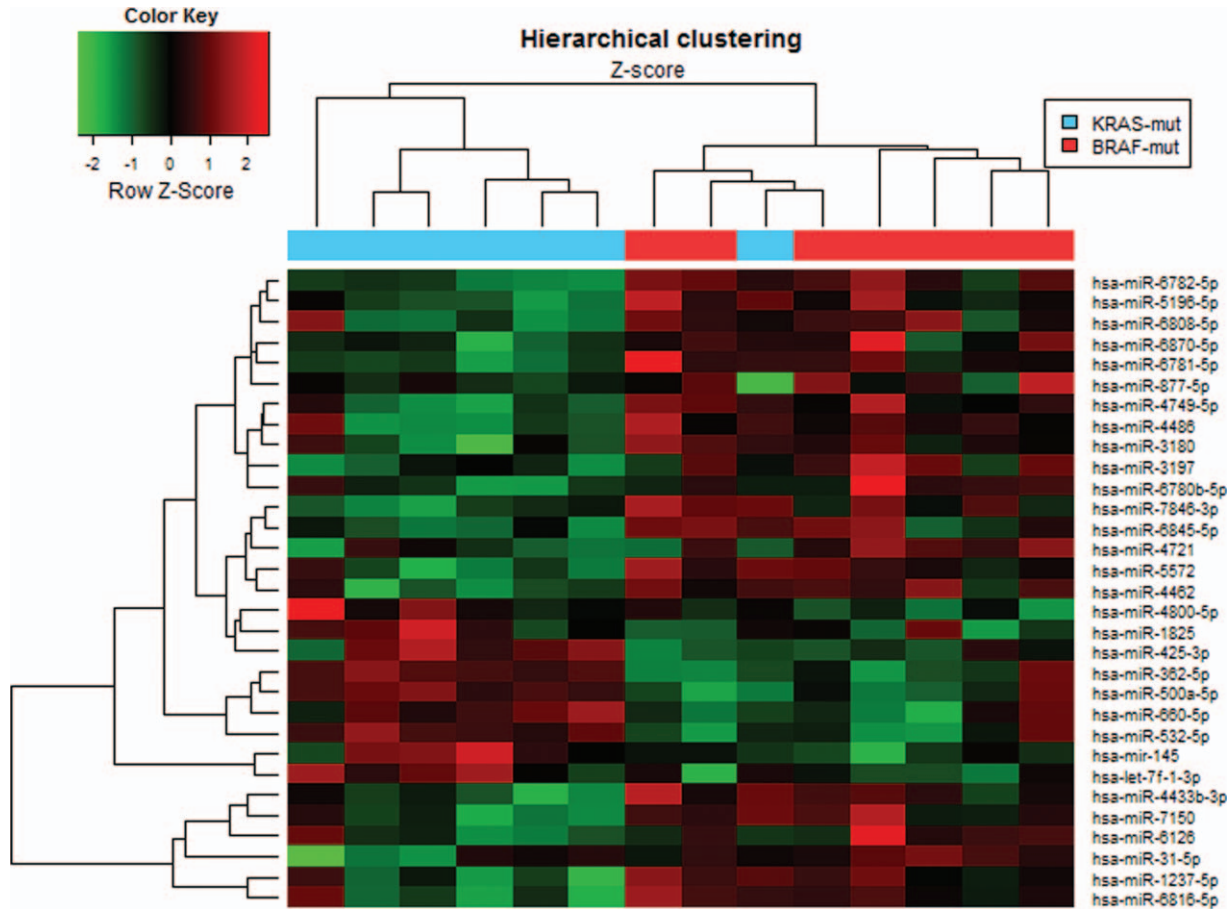


FIGURE 2. Unsupervised hierarchical clustering using differentially expressed miRNAs in *BRAF*-mutated versus *KRAS*-mutated colorectal cancers.

mutated cancers (Table 4). These encompassed the well-known cancer-associated signaling pathways including the neutrophin signaling pathway (FDR = 0.0128), pathways in cancer (FDR = 0.0968), Wnt signaling pathway (FDR = 0.1233), and MAPK signaling pathway (FDR = 0.1089). Pathways associated with cell adhesion such as adherens junction (FDR = 0.3387), ECM–receptor interaction (FDR = 0.3127), tight junction (FDR = 0.4342), and focal adhesion (FDR = 0.4319) were also enriched by DE-miRNAs

in *BRAF*-mutated CRCs, although they were not that significant.

DISCUSSION

In search for the different miRNA signatures associated with *BRAF*-mutated CRCs compared with *KRAS*-mutated CRCs, we applied strict criteria for tissue selection, and could identify different miRNA expression signature associated with the *BRAF* mutation. Although a recent study investigated the

TABLE 2. Significantly Altered miRNAs in *BRAF*-Mutated Compared With *KRAS*-Mutated CRCs by miRNA Array Analysis

| Name of miRNA (miR Base ID) | Accession | Fold Change | P | Expression |
|-----------------------------|--------------|-------------|--------|------------|
| hsa-let-7f-1-3p | MIMAT0004486 | −1.5619 | 0.0137 | Under |
| hsa-miR-31-5p | MIMAT0000089 | 8.3331 | 0.0365 | Over |
| hsa-miR-362-5p | MIMAT0000705 | −2.2877 | 0.0117 | Under |
| hsa-miR-425-3p | MIMAT0001343 | −1.6988 | 0.0313 | Under |
| hsa-miR-500a-5p | MIMAT0004773 | −2.1671 | 0.0334 | Under |
| hsa-miR-532-5p | MIMAT0002888 | −2.3266 | 0.0101 | Under |
| hsa-miR-660-5p | MIMAT0003338 | −1.8515 | 0.0454 | Under |
| hsa-miR-877-5p | MIMAT0004949 | 1.5248 | 0.0430 | Over |
| hsa-miR-1237-5p | MIMAT0022946 | 1.6144 | 0.0454 | Over |
| hsa-miR-1825 | MIMAT0006765 | −1.8155 | 0.0403 | Under |

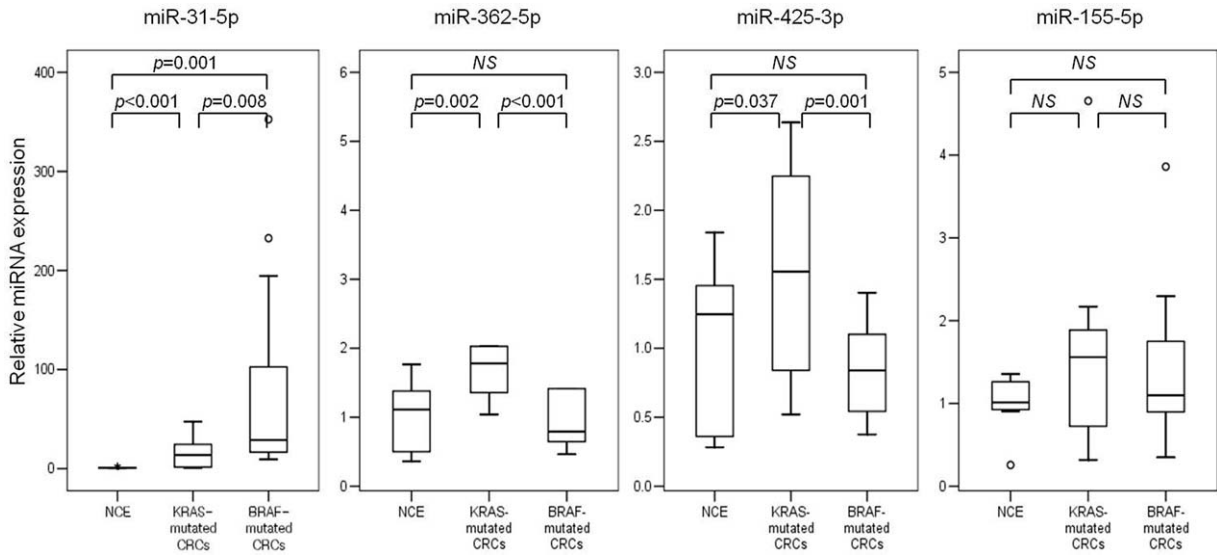


FIGURE 3. Box plots for the expression of selected microRNAs using quantitative reverse transcription polymerase chain reaction (qRT-PCR). CRC = colorectal cancers; NCE = normal colon epithelium.

different miRNA expression profiles in *BRAF*-mutated CRCs,²³ this study compared the miRNA expressions only according to the presence or absence of *BRAF* mutation. In addition, there has been no such study comparing the miRNA expression profiles associated with *BRAF* mutation in comparison to *KRAS* mutation. Furthermore, unlike other previous studies, we tried to minimize possible factors that could affect the expression of miRNAs, such as histology and MSI status. From our analysis, we obtained a total of 10 DE-miRNAs. These included 3

upregulated miRNAs and 7 downregulated miRNAs. Among these, miR-31-5p showed the most significant fold change (FC = 8.331), and this result was in accordance with that of a previous study,²³ thus further supporting the validity of our results.

In the analysis of the GO biologic processes, DE-miRNAs exert regulatory effect on target genes functionally associated with cellular proliferation such as positive regulation of gene expression, transcription, and RNA metabolic process. These

TABLE 3. Enriched Gene Functions Affected by Significantly Altered miRNAs in *BRAF*-Mutated Colorectal Cancer in Comparison to *KRAS*-Mutated Colorectal Cancer

| GO Term | P | Fold Enrichment | FDR |
|--|------------------------|-----------------|-----------------------|
| GO:0010628~positive regulation of gene expression | 1.26×10^{-10} | 1.736 | 5.00×10^{-7} |
| GO:0045941~positive regulation of transcription | 2.68×10^{-10} | 1.733 | 5.34×10^{-7} |
| GO:0045935~positive regulation of nucleobase, nucleoside, nucleotide, and nucleic acid metabolic process | 2.97×10^{-10} | 1.690 | 3.94×10^{-7} |
| GO:0006350~transcription | 9.70×10^{-10} | 1.326 | 9.65×10^{-7} |
| GO:0045893~positive regulation of transcription, DNA-dependent | 1.19×10^{-9} | 1.775 | 9.49×10^{-7} |
| GO:0051254~positive regulation of RNA metabolic process | 1.97×10^{-9} | 1.760 | 1.31×10^{-6} |
| GO:0045449~regulation of transcription | 2.11×10^{-9} | 1.278 | 1.20×10^{-6} |
| GO:0051173~positive regulation of nitrogen compound metabolic process | 2.70×10^{-9} | 1.637 | 1.34×10^{-6} |
| GO:0010557~positive regulation of macromolecule biosynthetic process | 4.06×10^{-9} | 1.624 | 1.80×10^{-6} |
| GO:0010604~positive regulation of macromolecule metabolic process | 6.46×10^{-9} | 1.527 | 2.57×10^{-6} |
| GO:0009891~positive regulation of biosynthetic process | 2.07×10^{-8} | 1.573 | 7.48×10^{-6} |
| GO:0031328~positive regulation of cellular biosynthetic process | 2.59×10^{-8} | 1.573 | 8.57×10^{-6} |
| GO:0006357~regulation of transcription from RNA polymerase II promoter | 1.21×10^{-7} | 1.525 | 3.71×10^{-5} |
| GO:0045944~positive regulation of transcription from RNA polymerase II promoter | 3.06×10^{-7} | 1.743 | 8.69×10^{-5} |
| GO:0051252~regulation of RNA metabolic process | 2.87×10^{-6} | 1.269 | 7.60×10^{-4} |
| GO:0006355~regulation of transcription, DNA-dependent | 8.19×10^{-6} | 1.259 | 2.03×10^{-3} |
| GO:0006351~transcription, DNA-dependent | 1.36×10^{-5} | 1.713 | 3.18×10^{-3} |
| GO:0032774~RNA biosynthetic process | 2.14×10^{-5} | 1.690 | 4.71×10^{-3} |
| GO:0016055~Wnt receptor signaling pathway | 2.55×10^{-5} | 2.084 | 5.32×10^{-3} |

FDR = false discovery rate.

TABLE 4. Significantly Deleterious Pathways by Altered miRNAs in BRAF-Mutated Colorectal Cancer in Comparison to KRAS-Mutated Colorectal Cancer

| Term—KEGG_PATHWAY | P | Fold Enrichment | FDR |
|--|-----------------------|-----------------|--------|
| hsa04722: neurotrophin signaling pathway | 6.84×10^{-5} | 2.053 | 0.0128 |
| hsa04062: chemokine signaling pathway | 7.16×10^{-4} | 1.691 | 0.0654 |
| hsa05200: pathways in cancer | 0.0016 | 1.458 | 0.0968 |
| hsa04310: Wnt signaling pathway | 0.0027 | 1.686 | 0.1233 |
| hsa04710: circadian rhythm | 0.0035 | 4.154 | 0.1246 |
| hsa04010: MAPK signaling pathway | 0.0036 | 1.473 | 0.1089 |
| hsa04120: ubiquitin-mediated proteolysis | 0.0152 | 1.577 | 0.3397 |
| hsa04520: adherens junction | 0.0173 | 1.803 | 0.3387 |
| hsa04666: Fc gamma R-mediated phagocytosis | 0.017 | 1.705 | 0.3080 |
| hsa04512: ECM–receptor interaction | 0.0196 | 1.745 | 0.3127 |
| hsa05130: pathogenic <i>Escherichia coli</i> infection | 0.0272 | 1.895 | 0.3783 |
| hsa04530: tight junction | 0.0355 | 1.497 | 0.4342 |
| hsa04510: focal adhesion | 0.0381 | 1.382 | 0.4319 |
| hsa05210: colorectal cancer | 0.0382 | 1.653 | 0.4091 |
| hsa04670: leukocyte transendothelial migration | 0.0468 | 1.504 | 0.4538 |

FDR = false discovery rate.

indicate that these altered miRNAs may generate growth signals in tumor cells and make them proliferate vigorously. In line with this, DE-miRNAs were significantly related to the signaling pathways implicated in cancer development and proliferation, such as pathways in cancer, Wnt signaling, and MAPK signaling. These findings also at least in part explain the much more aggressive biologic behavior of BRAF-mutated CRCs than KRAS-mutated CRCs. In particular, MAPK pathway (also known as the RAS-RAF-MEK-ERK signaling pathway) is classically thought to be activated by mutations in KRAS or BRAF in CRCs, but our results suggest that these DE-miRNAs may also regulate the MAPK pathway, leading to differential activity of the corresponding pathway. In addition, these miRNAs also regulate genes associated with cell adhesion including adherens junction and focal adhesion which play critical roles in tumor progression and metastasis.³³ Taken together, the DE-miRNAs in BRAF-mutated CRCs appear to be strongly involved in the aggressive phenotype of BRAF-mutated CRCs, and might be the potential treatment targets.

Among the DE-miRNAs, there is emerging evidence that miR-31-5p is closely associated with BRAF mutation in CRCs.^{23,26} Nosho et al²³ revealed that miR-31-5p was the most upregulated gene in BRAF-mutated CRCs compared with the BRAF wild-type group. They also demonstrated that high miR-31 expression was associated with MSI-high, proximal location, and worse cancer-specific survival.²³ Furthermore, a significant decrease of BRAF target proteins was demonstrated regardless of the mutational status after transfection of the miR-31 inhibitor in colon cancer cell lines.²³ Therefore, miR-31 may be a promising diagnostic biomarker and the therapeutic target in patients with CRC. Beside miR-31-5p, the function of other miRNAs in our list has not been investigated yet in CRCs in other studies. However, a number of these miRNAs have been implicated for tumorigenesis and metastasis in other cancer types. For example, it was demonstrated that miR-362-5p inhibited proliferation and migration of neuroblastoma cells by targeting phosphatidylinositol 3-kinase-C2 β ,³⁴ and that decreased expression of miR-425-3p was correlated with a worse prognosis in patients with hepatocellular carcinoma treated with sorafenib.³⁵ It has also been found that miR-

877-5p was upregulated in metastatic melanoma.³⁶ As such, the DE-miRNAs associated with the BRAF-mutated CRC cases merit further investigation as to the details of their specific function in this cancer type.

We should note that there were some limitations to the present study. Although we demonstrated a significant enrichment of dysregulated miRNAs in various cancer-related pathways in patients with BRAF-mutated CRC, we did not further validate their expression, nor demonstrated their specific roles in these pathways using functional experiments. Moreover, the low incidence of BRAF mutation in our CRC cases and our strict criteria for selecting cases resulted in small number of samples in this study. Also, the present results were obtained based on microarray analysis and bioinformatics prediction, and needed to be further validated in the future. Nonetheless, this study may be regarded as a preliminary analysis to provide valuable research direction for future studies, especially for treatment of CRCs.

In summary, we identified a specific miRNA expression signature associated with BRAF mutation in comparison to KRAS mutation in CRCs, and identified 10 DE-miRNAs including miR-31-5p, miR-362-5p, and miR-425-3p. These miRNAs were functionally associated with positive regulation of gene expression and transcription, and they exert a regulatory effect on target genes in known major cancer-related pathways such as Wnt and MAPK signaling pathways. Our results suggest that these DE-miRNAs are implicated for the aggressive phenotype of BRAF-mutated CRCs. Further experimental validation is required to confirm these results.

REFERENCES

1. Siegel R, Naishadham D, Jemal A. Cancer statistics, 2013. *CA Cancer J Clin.* 2013;63:11–30.
2. Kraus S, Nabiochtchikov I, Shapira S, et al. Recent advances in personalized colorectal cancer research. *Cancer Lett.* 2014;347:15–21.
3. Cunningham D, Humblet Y, Siena S, et al. Cetuximab monotherapy and cetuximab plus irinotecan in irinotecan-refractory metastatic colorectal cancer. *N Engl J Med.* 2004;351:337–345.

4. Karapetis CS, Khambata-Ford S, Jonker DJ, et al. K-ras mutations and benefit from cetuximab in advanced colorectal cancer. *N Engl J Med*. 2008;359:1757–1765.
5. Di Nicolantonio F, Martini M, Molinari F, et al. Wild-type BRAF is required for response to panitumumab or cetuximab in metastatic colorectal cancer. *J Clin Oncol*. 2008;26:5705–5712.
6. Yuan ZX, Wang XY, Qin QY, et al. The prognostic role of BRAF mutation in metastatic colorectal cancer receiving anti-EGFR monoclonal antibodies: a meta-analysis. *PLoS One*. 2013;8:e65995.
7. Baldus SE, Schaefer KL, Engers R, et al. Prevalence and heterogeneity of KRAS, BRAF, and PIK3CA mutations in primary colorectal adenocarcinomas and their corresponding metastases. *Clin Cancer Res*. 2010;16:790–799.
8. Brink M, de Goeij AF, Weijenberg MP, et al. K-ras oncogene mutations in sporadic colorectal cancer in The Netherlands Cohort Study. *Carcinogenesis*. 2003;24:703–710.
9. Weisenberger DJ, Siegmund KD, Campan M, et al. CpG island methylator phenotype underlies sporadic microsatellite instability and is tightly associated with BRAF mutation in colorectal cancer. *Nat Genet*. 2006;38:787–793.
10. Lochhead P, Kuchiba A, Imamura Y, et al. Microsatellite instability and BRAF mutation testing in colorectal cancer prognostication. *J Natl Cancer Inst*. 2013;105:1151–1156.
11. Kawazoe A, Shitara K, Fukuoka S, et al. A retrospective observational study of clinicopathological features of KRAS, NRAS, BRAF and PIK3CA mutations in Japanese patients with metastatic colorectal cancer. *BMC Cancer*. 2015;15:258.
12. Yuen ST, Davies H, Chan TL, et al. Similarity of the phenotypic patterns associated with BRAF and KRAS mutations in colorectal neoplasia. *Cancer Res*. 2002;62:6451–6455.
13. Ahlquist T, Bottillo I, Danielsen SA, et al. RAS signaling in colorectal carcinomas through alteration of RAS, RAF, NF1, and/or RASSF1A. *Neoplasia*. 2008;10:680–686; 682 p following 686.
14. Pai RK, Jayachandran P, Koong AC, et al. BRAF-mutated, microsatellite-stable adenocarcinoma of the proximal colon: an aggressive adenocarcinoma with poor survival, mucinous differentiation, and adverse morphologic features. *Am J Surg Pathol*. 2012;36:744–752.
15. Roth AD, Tejpar S, Delorenzi M, et al. Prognostic role of KRAS and BRAF in stage II and III resected colon cancer: results of the translational study on the PETACC-3, EORTC 40993, SAKK 60-00 trial. *J Clin Oncol*. 2010;28:466–474.
16. Ogino S, Meyerhardt JA, Irahara N, et al. KRAS mutation in stage III colon cancer and clinical outcome following intergroup trial CALGB 89803. *Clin Cancer Res*. 2009;15:7322–7329.
17. Huntzinger E, Izaurralde E. Gene silencing by microRNAs: contributions of translational repression and mRNA decay. *Nat Rev Genet*. 2011;12:99–110.
18. Volinia S, Calin GA, Liu CG, et al. A microRNA expression signature of human solid tumors defines cancer gene targets. *Proc Natl Acad Sci USA*. 2006;103:2257–2261.
19. Schetter AJ, Heegaard NH, Harris CC. Inflammation and cancer: interweaving microRNA, free radical, cytokine and p53 pathways. *Carcinogenesis*. 2010;31:37–49.
20. Lu J, Getz G, Miska EA, et al. MicroRNA expression profiles classify human cancers. *Nature*. 2005;435:834–838.
21. Yanaihara N, Caplen N, Bowman E, et al. Unique microRNA molecular profiles in lung cancer diagnosis and prognosis. *Cancer Cell*. 2006;9:189–198.
22. Rossi S, Di Narzo AF, Mestdagh P, et al. microRNAs in colon cancer: a roadmap for discovery. *FEBS Lett*. 2012;586:3000–3007.
23. Nosho K, Igarashi H, Nojima M, et al. Association of microRNA-31 with BRAF mutation, colorectal cancer survival and serrated pathway. *Carcinogenesis*. 2014;35:776–783.
24. Ma Y, Zhang P, Wang F, et al. miR-150 as a potential biomarker associated with prognosis and therapeutic outcome in colorectal cancer. *Gut*. 2012;61:1447–1453.
25. Mosakhani N, Sarhadi VK, Borze I, et al. MicroRNA profiling differentiates colorectal cancer according to KRAS status. *Genes Chromosomes Cancer*. 2012;51:1–9.
26. Ito M, Mitsuhashi K, Igarashi H, et al. MicroRNA-31 expression in relation to BRAF mutation, CpG island methylation and colorectal continuum in serrated lesions. *Int J Cancer*. 2014;135:2507–2515.
27. American Joint Committee on Cancer. AJCC cancer staging manual. 7th ed. New York: Springer; 2010.
28. Kwon MJ, Jeon JY, Park HR, et al. Low frequency of KRAS mutation in pancreatic ductal adenocarcinomas in Korean patients and its prognostic value. *Pancreas*. 2015;44:484–492.
29. Sargent DJ, Marsoni S, Monges G, et al. Defective mismatch repair as a predictive marker for lack of efficacy of fluorouracil-based adjuvant therapy in colon cancer. *J Clin Oncol*. 2010;28:3219–3226.
30. Shahab SW, Matyunina LV, Mezencev R, et al. Evidence for the complexity of microRNA-mediated regulation in ovarian cancer: a systems approach. *PLoS One*. 2011;6:e22508.
31. Nam JW, Rissland OS, Koppstein D, et al. Global analyses of the effect of different cellular contexts on microRNA targeting. *Mol Cell*. 2014;53:1031–1043.
32. Yuen T, Ruf F, Chu T, et al. Microtranscriptome regulation by gonadotropin-releasing hormone. *Mol Cell Endocrinol*. 2009;302:12–17.
33. Zhao J, Guan JL. Signal transduction by focal adhesion kinase in cancer. *Cancer Metastasis Rev*. 2009;28:35–49.
34. Wu K, Yang L, Chen J, et al. miR-362-5p inhibits proliferation and migration of neuroblastoma cells by targeting phosphatidylinositol 3-kinase-C2beta. *FEBS Lett*. 2015;589:1911–1919.
35. Vaira V, Roncalli M, Carnaghi C, et al. MicroRNA-425-3p predicts response to sorafenib therapy in patients with hepatocellular carcinoma. *Liver Int*. 2015;35:1077–1086.
36. Qi M, Huang X, Zhou L, et al. Identification of differentially expressed microRNAs in metastatic melanoma using next-generation sequencing technology. *Int J Mol Med*. 2014;33:1117–1121.